Supporting Information

Achieving Persistent Room-Temperature Phosphorescence from Phenanthridone Derivatives by Molecular Engineering

Hongzhuo Wu, Deliang Wang, Jianquan Zhang, Parvej Alam, Zheng Zhao, Yu Xiong, Dong Wang, and Ben Zhong Tang**

Table of Contents

1. General methods

All the reactions were carried out under a nitrogen atmosphere. The 6(5H)-Phenanthridinone, halogen-substituted benzyl bromide and reagents of CuCN, K_2CO_3, N-Bromosuccinimide, N-chlorosuccinimide were purchased from commercial suppliers and used directly without further purification. ^{1}H NMR spectra were recorded on a Varian Mercury 400 NMR spectrometer in $CDCl_3$ using *tetra*-methylsilane as the internal standard. ^{13}C NMR spectra were recorded on the Bruker AVANCE III HD 600 MHz NMR spectrometer in $CDCl_3$ using *tetra*-methylsilane as the internal standard. High-resolution mass spectra were recorded on a thermo scientific Q-exactive focus (FTMS + pESI) mass spectrometer. High-performance liquid chromatography (HPLC)

was performed on the Waters e2695 HPLC system using an XBridge^{TM}-C18 column (5 mm). The running buffer was 10%H_2O-90%MeOH. The UV-*vis* absorption spectra were recorded on a UV-2600 spectrophotometer, and the photoluminescence spectra were recorded on a PerkinElmer LS55 fluorescence spectrometer. Absolute quantum yields were measured by integrating sphere on a Quantaurus-QY plus (Hamamatsu C11347-11) spectrofluorometer. The lifetimes were measured on an Edinburgh FLS1000 fluorescence spectrophotometer equipped with a continuous xenon lamp (Xe1), a microsecond pulsed xenon flashlamp (uF920), and a nanosecond flashlamp lamp (nF920), respectively. Single crystal data were collected on a Bruker Smart APEXII CCD diffractometer using graphite monochromated Mo Kα radiation (λ = 0.71073 Å) or Cu Kα radiation (λ = 1.54184 Å). Elemental analysis was performed on an EL cube. The photos and videos were recorded by a Nikon 7200.

Mean decay times (τ_p) were obtained from individual lifetimes τ_i and amplitudes a_i of multi-exponential evaluation by the below equation:

$$\tau_p = \frac{\sum_i a_i \tau_i^2}{\sum_i a_i \tau_i}$$

2. Density functional theory calculations

The geometries of all compounds in isolated gas state were optimized by density functional theory (DFT) using the B3LYP density functional and 6-31G (d, p) basis set. Analytical frequency calculations were also carried out at the same level of theory to confirm that the optimized structures are located at a minimum point. The quantum mechanics/molecular mechanics (QM/MM) theory with tow-layer ONIOM method[1] was implemented to calculated the aggregation effect and vertical excitation energies of Sn and Tn in the crystal at the B3LYP/6-31G (d, p) level. The computational models were built by digging a 3×3×3 supercell from X-ray crystal structure without further optimization, and the central molecule acts as the QM part (high layer) and the surrounding molecules are treated as MM part (low layer), as shown in **Chart S1~ 6**. The universal force field (UFF) was used for the MM expressions. The above-mentioned quantum chemical calculations were carried out by using Gaussian 09[2]. Spin-orbital coupling matrix elements of structures in gas state and crystal were investigated by ORCA program (Version 5.0.3).

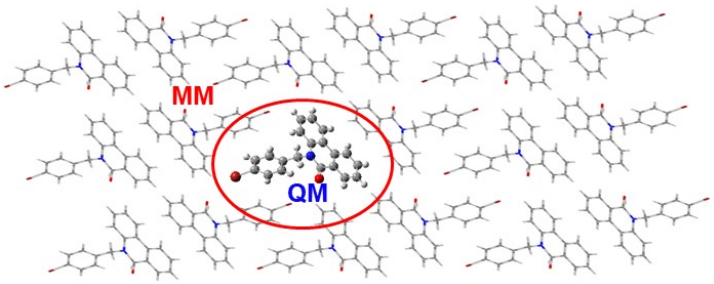

Chart S1. QM/MM model of PTD-BnBr: one central QM molecule for the higher layer and the surrounding MM molecules for the lower layer.

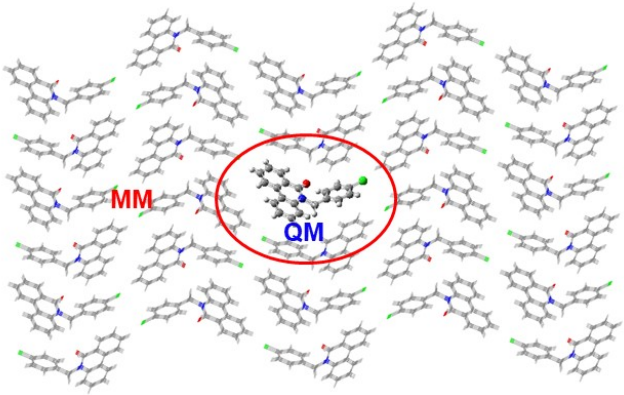

Chart S2. QM/MM model of PTD-BnCl: one central QM molecule for the higher layer and the surrounding MM molecules for the lower layer.

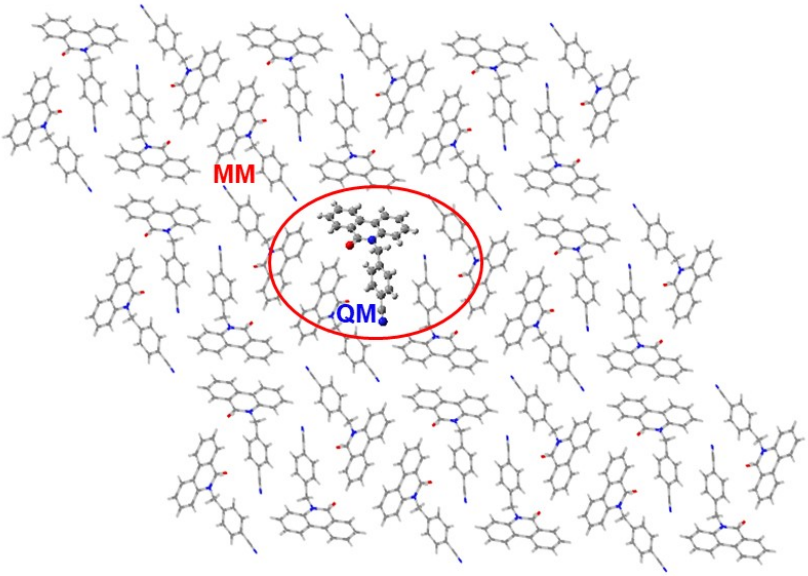

Chart S3. QM/MM model of PTD-BnCN: one central QM molecule for the higher layer and the surrounding MM molecules for the lower layer.

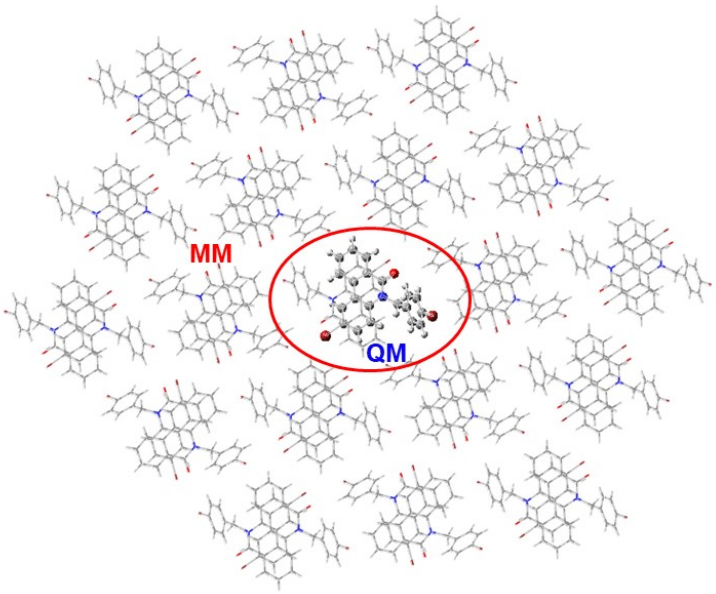

Chart S4. QM/MM model of Br-PTD: one central QM molecule for the higher layer and the surrounding MM molecules for the lower layer.

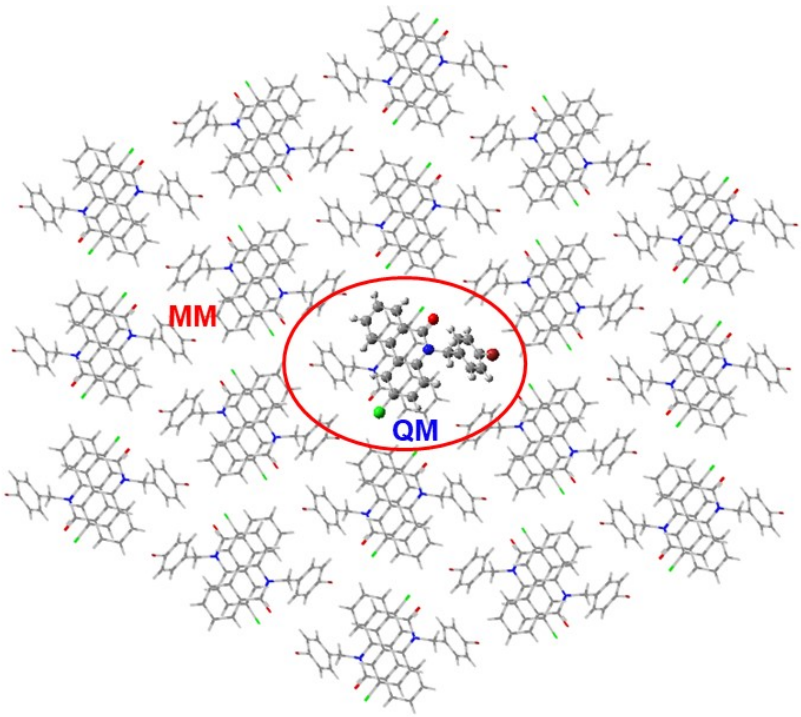

Chart S5. QM/MM model of Cl-PTD: one central QM molecule for the higher layer and the surrounding MM molecules for the lower layer.

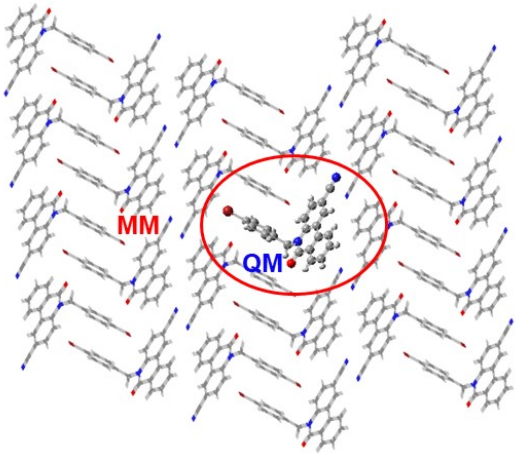

Chart S6. QM/MM model of CN-PTD: one central QM molecule for the higher layer and the surrounding MM molecules for the lower layer.

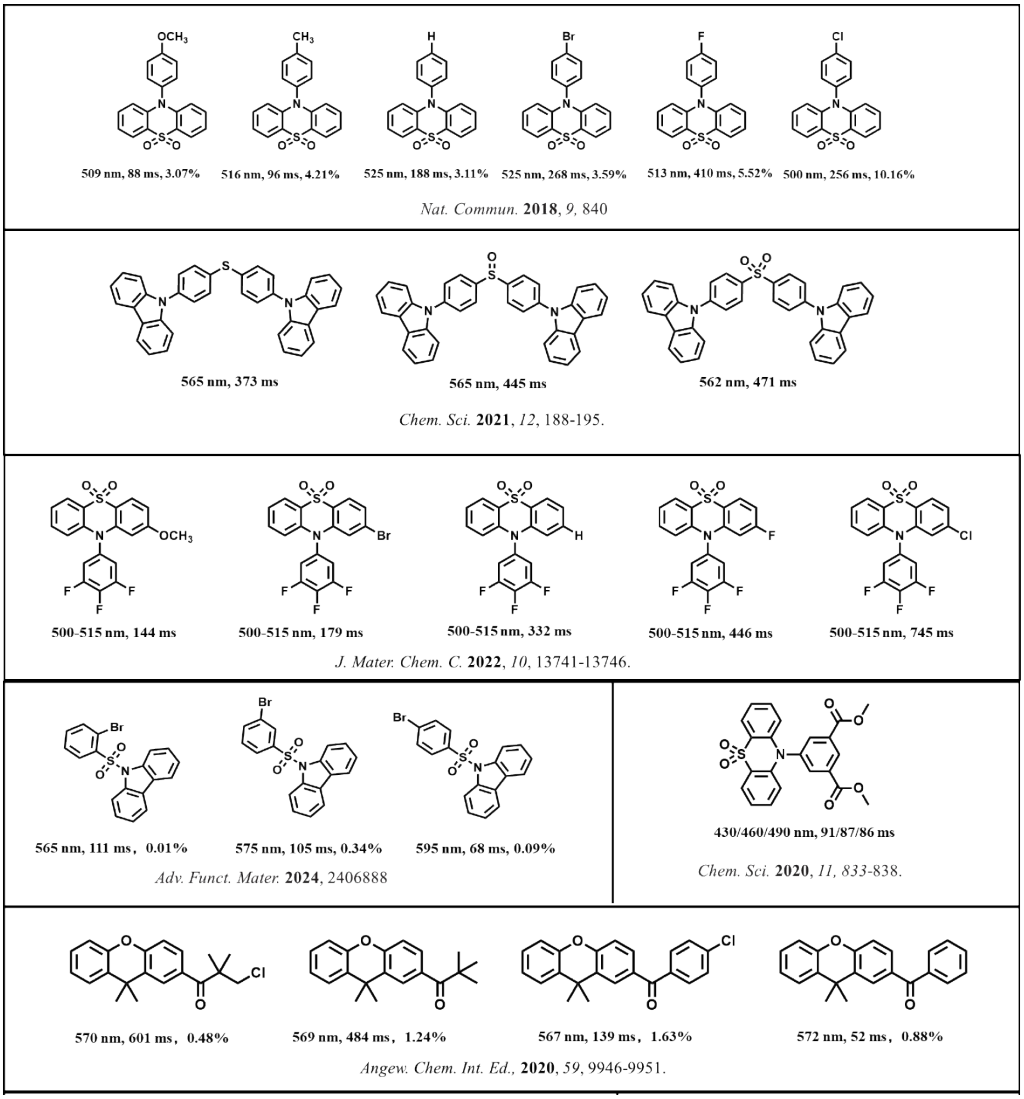

648 nm, 0.59 ms，3.7%

629 nm, 0.23 ms，1.8%

559 nm, 0.11 ms，1.6%

J. Mater. Chem. C. **2023**, *11*, 3003-3009.

559 nm, 0.048 ms，35%

549 nm, 0.706 ms，36.56%

Nat. Commun. **2018**, *9*, 2963.

585 nm, 0.61 ms，48%

576 nm, 11.4 ms，26%

Angew. Chem. Int. Ed., **2021**, *60*, 12323.

552 nm, 2.15 ms

540 nm, 3.15 ms

575 nm, 570 ms

J. Mater. Chem. C. **2021**, *9*, 727-735.

555-616 nm, 210 ms，6.2%

555-616 nm, 200 ms，3.3%

555-616 nm, 110 ms，2.7%

590 nm, 8.14 ms，6.3%

Chem. Sci. **2021**, *12*, 15116-15127.

524 nm, 680 ms，0.3%

540/575 nm, 480 ms，1.2%

Angew. Chem. Int. Ed., **2020**, *59*, 17137-17144.

465 nm, 1790 ms

500 nm, 1820 ms，2.0%

J. Am. Chem. Soc. **2017**, *139*, 2728-2733

640 nm, 0.13 ms

655 nm, 0.56 ms

647 nm, 0.58 ms

J. Am. Chem. Soc. **2019**, *141*, 5045.

596 nm, 436 ms

Angew. Chem. Int. Ed., **2020**, *59*, 4756-4762.

505 nm, 745 ms, 31.2%

521 nm, 551 ms，0.2%

430 nm, 2450 ms, 7.2%

Nat. Photonics. **2019**, *13*, 406-411.

530 nm, 234 ms，4.1%

520 nm, 322 ms，8.44%

510 nm, 323 ms, 1.61%

Adv. Optical Mater. **2023**, *11*, 2202904

635 nm, 344 ms

640 nm, 285 ms

660 nm, 296 ms

Adv. Mater. **2022**, *34*, 2201280.

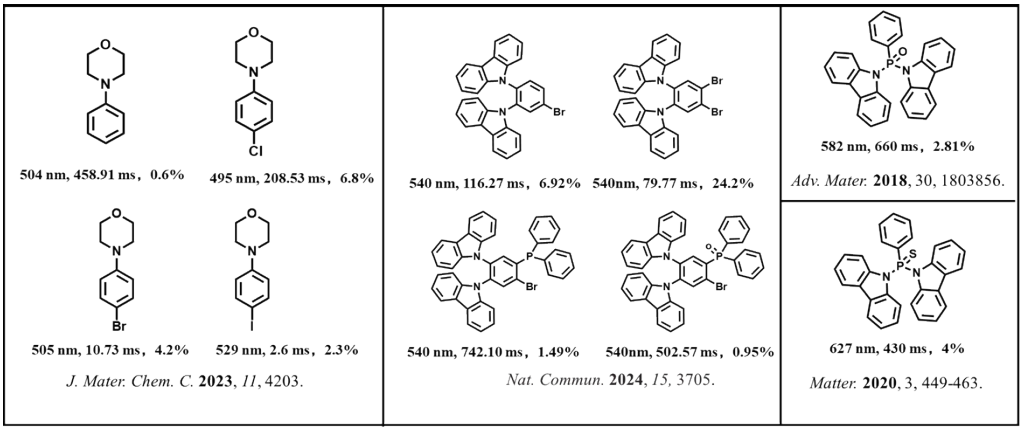

Scheme S1. Representative organic small molecular RTP materials reported in recent years (RTP properties including the emission wavelength, lifetime, and phosphorescence quantum efficiency were obtained from powders or crystals under ambient conditions).

3. Synthesis of target compounds

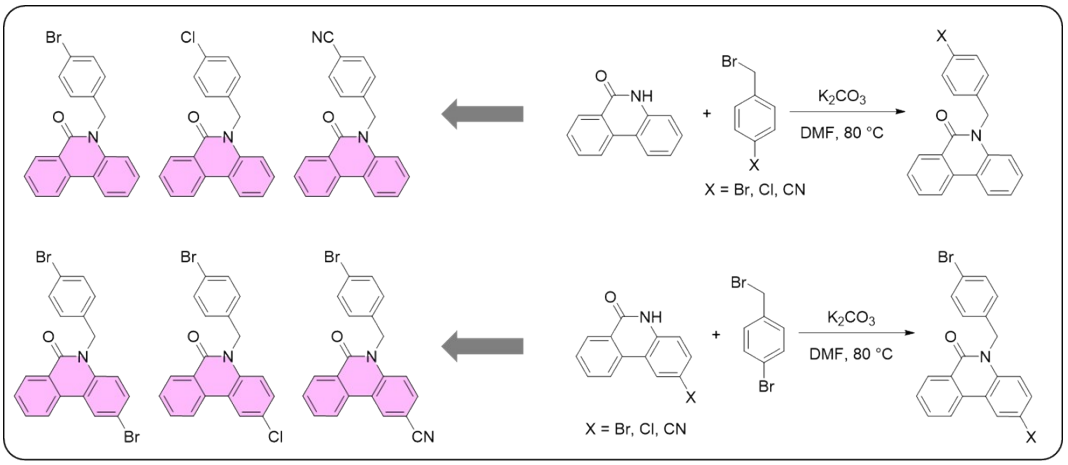

Scheme S2. General synthetic routes of PTD derivatives PTD-BnBr, PTD-BnCl, PTD-BnCN, Br-PTD, Cl-PTD, and CN-PTD.

3.1 General synthetic procedure of PTD-BnBr, PTD-BnCl and PTD-BnCN

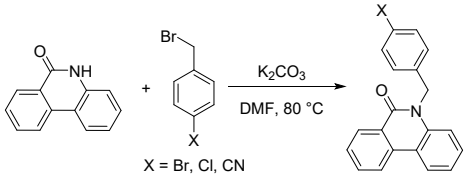

Scheme S3. The synthetic route of PTD-BnBr, PTD-BnCl and PTD-BnCN.

PTD-BnBr: 6(5H)-Phenanthridinone (0.78 g, 4.0 mmol), K_2CO_3 (1.66 g, 12.0 mmol) and anhydrous DMF (20 mL) were added into a 100 mL double-neck round-bottom

flask. The mixture was stirred at 100 ℃ for 1 h under a nitrogen stream. Then, 1-(bromomethyl)-4-bromobenzene (1.50 g, 6.0 mmol) was added, and the resulting mixture was heated at 70 ℃ for 8 h. After cooling to room temperature, water (20 mL) was poured into the reaction mixture, and stirred for 10 min. The resulting mixture was extracted by ethyl acetate for three times, then the combined organic layers were dried over anhydrous $MgSO_4$ and the solvent was removed under reduced pressure. The crude product was purified by silica gel column chromatography (eluent: petroleum ether/CH_2Cl_2 = 2:1), followed by recrystallization for two times from chloroform/methanol to get colorless crystals (yield: 1.04 g, 71.0%). ^{1}H NMR ($CDCl_3$, 400 MHz) δ (ppm): 5.52 (s, 2H), 7.06 (d, J = 8.4 Hz, 2H), 7.24 – 7.11 (m, 2H), 7.32 (m, 3H), 7.54 (t, J = 7.6 Hz, 1H), 7.72 (t, J = 7.7 Hz, 1H), 8.22 (m, 2H), 8.53 (m,1H). ^{13}C NMR (151 MHz, $CDCl_3$) δ (ppm): 161.98, 137.19, 135.81, 133.92, 132.96, 132.02, 129.73, 129.27, 128.46, 128.26, 125.39, 123.54, 122.87, 121.86, 121.17, 119.68, 115.88, 46.07. HRMS (ESI) m/z: calcd for $C_{20}H_{14}BrNO$: 363.0259. Found: 364.03267 $(M+1)^+$. Elemental analysis calcd for $C_{20}H_{14}BrNO$: C, 65.95. H, 3.87. N, 3.85. Found: C, 65.56. H, 3.74. N, 3.58.

PTD-BnCl: Yield: 56.0%. ^{1}H NMR ($CDCl_3$, 400 MHz) δ (ppm): 5.63 (s, 2H), 7.21 (d, J = 8.6 Hz, 2H), 7.27 (m, 4H), 7.41 (m, 1H), 7.63 (t, J = 7.6 Hz, 1H), 7.81 (m, 1H), 8.31 (m, 2H), 8.62 (m,1H). ^{13}C NMR (101 MHz, $CDCl_3$) δ (ppm): 162.03, 137.27, 135.30, 133.97, 133.15, 132.99, 129.76, 129.33, 129.12, 128.29, 128.14, 125.46, 123.58, 122.89, 121.89, 119.74, 115.93, 46.06. HRMS (ESI) m/z: calcd for $C_{20}H_{14}ClNO$: 319.0764. Found: 320.08334 $(M+1)^+$. Elemental analysis calcd for $C_{20}H_{14}ClNO$: C, 75.12. H, 4.41. N, 4.38. Found: C, 75.00. H, 4.28. N, 4.28.

PTD-BnCN: Yield: 68.0%. ^{1}H NMR ($CDCl_3$, 500 MHz) δ (ppm): δ 5.71 (s, 2H), 7.16 (d, J = 8.4 Hz, 1H), 7.34 – 7.30 (m, 1H), 7.36 (d, J = 8.4 Hz, 2H), 7.40 – 7.43 m, 1H), 7.60 (d, J = 8.4 Hz, 2H), 7.67 – 7.62 (m, 1H), 7.85 – 7.80 (m, 1H), 8.33 (d, J = 8.1 Hz, 2H), 8.60 (dd, J = 8.0, 1.1 Hz, 1H). ^{13}C NMR (151 MHz, $CDCl_3$) δ (ppm): 162.02, 142.37, 137.02, 133.95, 133.20, 132.82, 129.87, 129.31, 128.43, 127.40, 125.25, 123.77, 123.14, 121.96, 119.79, 118.77, 115.60, 111.39, 46.36. HRMS (ESI) m/z: calcd for $C_{21}H_{14}N_2O$: 310.1106. Found: 311.11760 $(M+1)^+$. Elemental analysis calcd for $C_{21}H_{14}N_2O$: C, 81.27. H, 4.55. N, 9.03. Found: C, 80.84. H, 4.19. N, 8.74.

3.2 General synthetic procedure of Br-PTD, Cl-TPD, and CN-PTD

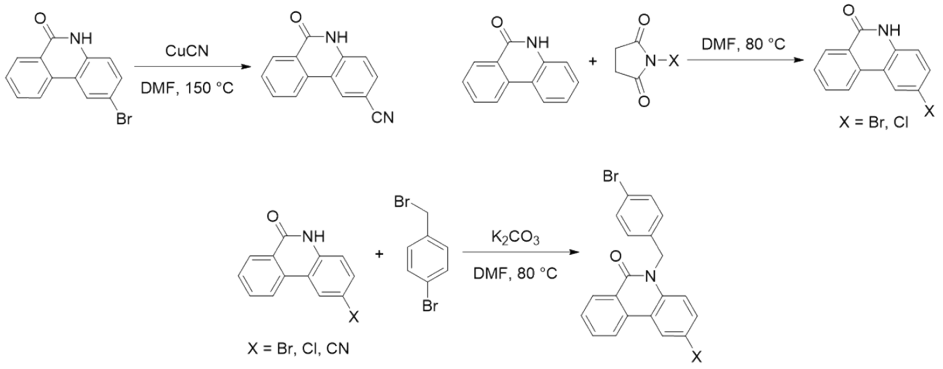

Scheme S4. Synthetic routes of compounds Br-PTD, Cl-PTD, and CN-PTD.

The compounds 2-bromophenanthridin-6(5H)-one, 2-chlorophenanthridin-6(5H)-one, and 2-cyanophenanthridin-6(5H)-one were prepared according to the previous literatures without any modification.[3-4]

Br-PTD: 2-bromophenanthridin-6(5H)-one (0.68 g, 2.5 mmol), K_2CO_3 (0.69 g, 5.0 mmol) and anhydrous DMF (20 mL) were added into a 50 mL double-neck round-bottom flask. The mixture was stirred at 100 ℃ for 1 h under a nitrogen stream. Then, 1-(bromomethyl)-4-bromobenzene (0.94 g, 3.75 mmol) was added and the solution was heated at 70 ℃ for 8 h. After cooling to room temperature, water (20 mL) was poured into the reaction mixture, and stirred for 10 min. The resulting mixture was extracted by ethyl acetate for three times, then the combined organic layers were dried over anhydrous $MgSO_4$ and the solvent was removed under reduced pressure. The crude product was purified by silica gel column chromatography (eluent: petroleum ether/CH_2Cl_2 = 2:1), followed by recrystallization for two times from chloroform/methanol to get colorless crystals (yield: 0.80 g, 72.6%). ^{1}H NMR ($CDCl_3$, 400 MHz) δ (ppm): 5.57 (s, 2H), 7.11 (dd, J = 8.6, 5.5 Hz, 3H), 7.42 (d, J = 8.4 Hz, 2H), 7.48 (dd, J = 9.0, 2.1 Hz, 1H), 7.66 (t, J = 7.6 Hz, 1H), 7.82 (t, J = 7.7 Hz, 1H), 8.23 (d, J = 8.2 Hz, 1H), 8.38 (d, J = 2.1 Hz, 1H), 8.60 (d, J = 8.0 Hz, 1H). ^{13}C NMR (151 MHz, $CDCl_3$) δ (ppm): 161.62, 136.13, 135.34, 133.20, 132.66, 132.37, 132.14, 129.40, 128.98, 128.38, 126.34, 125.54, 121.95, 121.48, 121.39, 117.55, 116.11, 46.13. HRMS (ESI) m/z: calcd for $C_{20}H_{13}Br_2NO$: 440.9364. Found: 441.9434 $(M+1)^+$. Elemental analysis calcd for $C_{20}H_{13}Br_2NO$: C, 54.21. H, 2.96. N, 3.16. Found: C, 54.45. H, 2.87. N, 3.08.

Cl-PTD: Yield: 79.0%. ^{1}H-NMR ($CDCl_3$, 500 MHz) (ppm): 5.58 (s, 2H), 7.12 (d, J = 8.4 Hz, 2H), 7.16 (d, J = 9.0 Hz, 1H), 7.35 (dd, J = 9.0, 2.3 Hz, 1H), 7.42 (d, J = 8.4 Hz, 2H), 7.70 – 7.63 (m, 1H), 7.85 – 7.80 (m, 1H), 8.26 – 8.21 (m, 2H), 8.60 (dd, J =

8.0, 1.3 Hz, 1H). ^{13}C NMR (101 MHz, $CDCl_3$) δ (ppm):161.67, 135.75, 135.40, 133.22, 132.79, 132.16, 129.59, 129.45, 128.99, 128.66, 128.40, 125.61, 123.37, 121.98, 121.41, 121.12, 117.28, 46.20. HRMS (ESI) m/z: calcd for $C_{20}H_{13}BrClNO$: 396.9869. Found: 397.9939 $(M+1)^+$. Elemental analysis calcd for $C_{20}H_{13}BrClNO$: C, 60.25. H, 3.29. N, 3.51. Found: C, 60.19. H, 3.00. N, 3.36.

CN-PTD: Yield: 76.9%. ^{1}H-NMR ($CDCl_3$, 500 MHz) (ppm): δ 5.59 (s, 2H), 7.11 (d, *J* = 8.4 Hz, 2H), 7.30 (d, *J* = 8.8 Hz, 1H), 7.43 (d, *J* = 8.4 Hz, 2H), 7.63 (dd, *J* = 8.8, 1.8 Hz, 1H), 7.71 (t, *J* = 7.5 Hz, 1H), 7.90 – 7.84 (m, 1H), 8.26 (d, *J* = 8.2 Hz, 1H), 8.56 (d, *J* = 1.6 Hz, 1H), 8.60 (dd, *J* = 8.0, 1.0 Hz, 1H). ^{13}C NMR (151 MHz, $CDCl_3$) δ (ppm): 161.75, 140.08, 134.77, 133.70, 132.41, 132.27, 132.23, 129.61, 129.53, 128.31, 128.13, 125.52, 121.95, 121.66, 120.31, 118.68, 116.69, 106.44, 46.28. HRMS (ESI) m/z: calcd for $C_{21}H_{13}BrN_2O$: 388.0211. Found: 389.0281 $(M+1)^+$. Elemental analysis calcd for $C_{21}H_{13}BrN_2O$: C, 64.80. H, 3.37. N, 7.20. Found: C, 64.89. H, 3.18. N, 7.10.

4. Supporting Figures and Tables

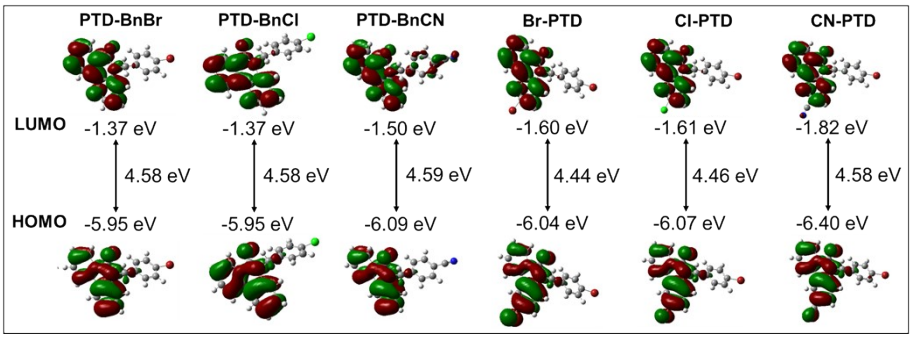

Figure S1. Calculated frontier molecular orbitals of PTD derivatives PTD-BnBr, PTD-BnCl, PTD-BnCN, Br-PTD, Cl-PTD, and CN-PTD in the gas phase.

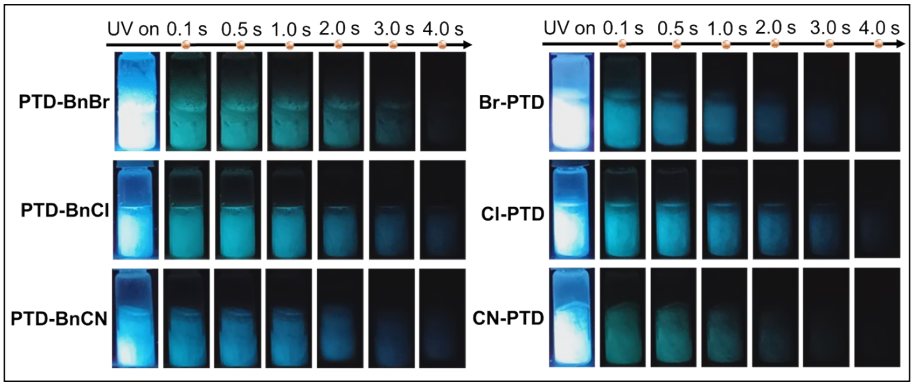

Figure S2. Luminescence photographs of PTD derivatives in dilute THF solutions (10^{-5} M) at 77 K under and after removing the UV irradiation (365 nm).

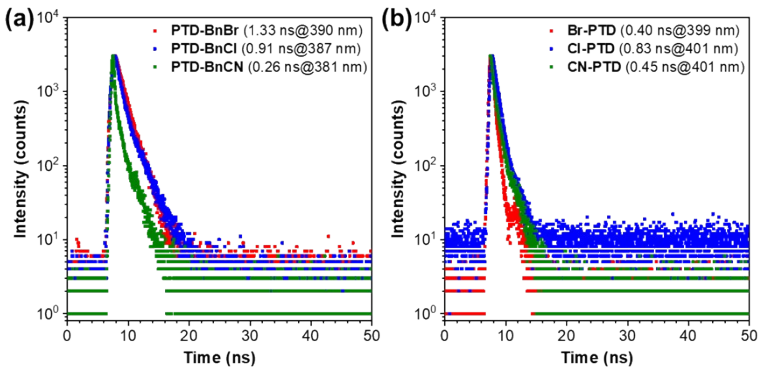

Figure S3. (a-b) Time-resolved fluorescence decay curves of PTD derivatives PTD-BnBr, PTD-BnCl, PTD-BnCN, Br-PTD, Cl-PTD, and CN-PTD in crystals.

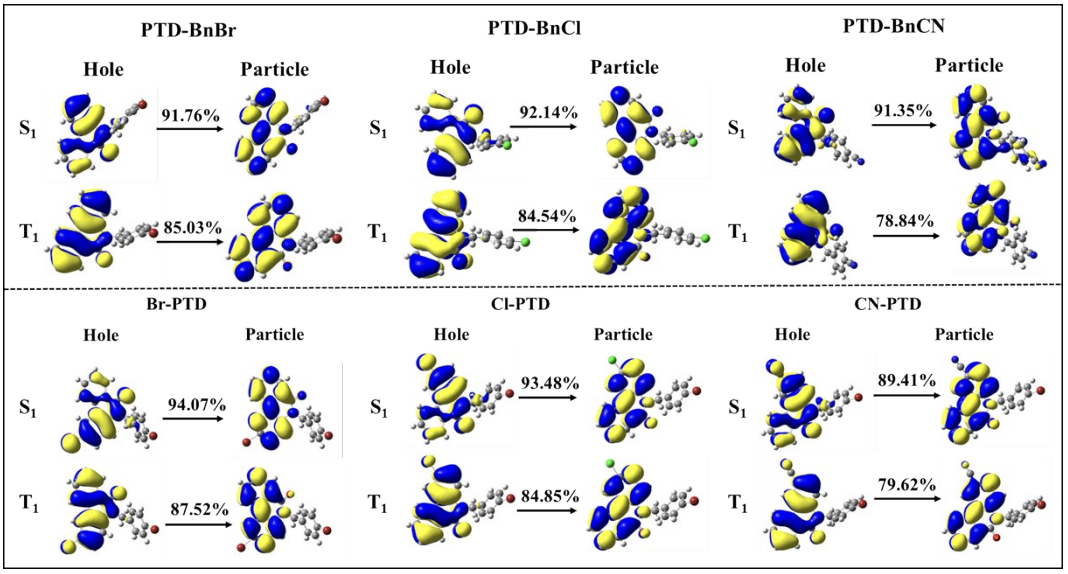

Figure S4. Calculated natural transition orbitals (NTOs) of S_1 and T_1 states of PTD-BnBr, PTD-BnCl, PTD-BnCN, Br-PTD, Cl-PTD, and CN-PTD in crystal phase.

Table S1. Calculated proportions of n→π* (α%) and π→π* (β%) configurations in the S_1 and T_1 states of PTD-BnBr, PTD-BnCl, PTD-BnCN, Br-PTD, Cl-PTD, and CN-PTD in the crystal state, respectively.

PTD derivatives	S_1		T_1	
	α%	β%	α%	β%
PTD-BnBr	1.65%	98.35%	0.27%	99.73%
PTD-BnCl	2.03%	97.97%	0.26%	99.74%
PTD-BnCN	1.79%	98.21%	0.17%	99.83%
Br-PTD	13.39%	86.61%	3.05%	96.95%
Cl-PTD	10.06%	89.94%	2.10%	97.90%
CN-PTD	1.79%	98.21%	0.25%	99.75%

Table S2. Single crystal data of compounds PTD-BnBr, PTD-BnCl, PTD-BnCN, Br-PTD, Cl-PTD and CN-PTD.

Name	PTD-BnBr	PTD-BnCl	PTD-BnCN	Br-PTD	Cl-PTD	CN-PTD
Crystal system	monoclinic	monoclinic	monoclinic	monoclinic	monoclinic	monoclinic
Space group	$P2_1$	$P2_1/n$	$P2_1$	$P2_1/n$	$P2_1/n$	$P2_1/c$
a/Å	8.3495(8)	5.6526(8)	18.334(4)	7.0974(6)	7.0938(7)	15.2781(10)
b/Å	5.1564(4)	25.098(3)	5.0895(10)	21.6508(15)	21.7282(19)	6.7491(4)
c/Å	18.3745(14)	11.1799(13)	18.931(4)	10.7738(8)	10.6282(9)	16.5330(10)
α/°	90	90	90	90	90	90
β/°	102.763(8)	101.355(14)	117.16(3)	97.688(8)	97.716(9)	100.120(6)
γ/°	90	90	90	90	90	90
Volume/Å^3	771.54(11)	1555.0(3)	1571.7(7)	1640.7(2)	1623.4(3)	1678.25(18)
Z	2	4	4	4	4	4
ρ_{calc}g/cm^3	1.568	1.366	1.312	1.794	1.631	1.541
μ/mm^{-1}	2.668	0.249	0.082	4.947	2.703	2.460
F(000)	368.0	664.0	648.0	872.0	800.0	784.0
h, k, lmax	11, 7, 25	6, 29, 13	21, 5, 22	8, 25, 12	8, 25, 12	18, 8, 19
Nref	4242[2346]	2738	5203[2932]	2895	2865	2943
Tmin,Tmax	0.518, 0.726	0.956, 0.973	0.991, 0.993	0.282, 0.476	0.479, 0.615	0.546, 0.744
R(reflections)	0.0443(2253)	0.0489(2106)	0.0583(2316)	0.0491(1991)	0.0579(1668)	0.0437(2068)
wR2(reflections)	0.0730(3448)	0.1058(2734)	0.0793(4800)	0.1024(2894)	0.0999(2865)	0.0865(2942)
Data completeness	1.47/0.81	0.999	1.64/0.92	1.000	1.000	1.000
Theta(max)	29.347	24.996	24.499	24.999	24.997	25.000
S	0.977	1.086	0.836	1.038	0.997	1.027
Npar	208	208	433	217	217	226

a) The single-crystal structures have been deposited at the Cambridge Crystallographic Data Centre and allocated the deposition number: PTD-BnBr (2342466), PTD-BnCl (2342465), PTD-BnCN (2342468), Br-PTD (2342463), Cl-PTD (2342464), CN-PTD (2342467).

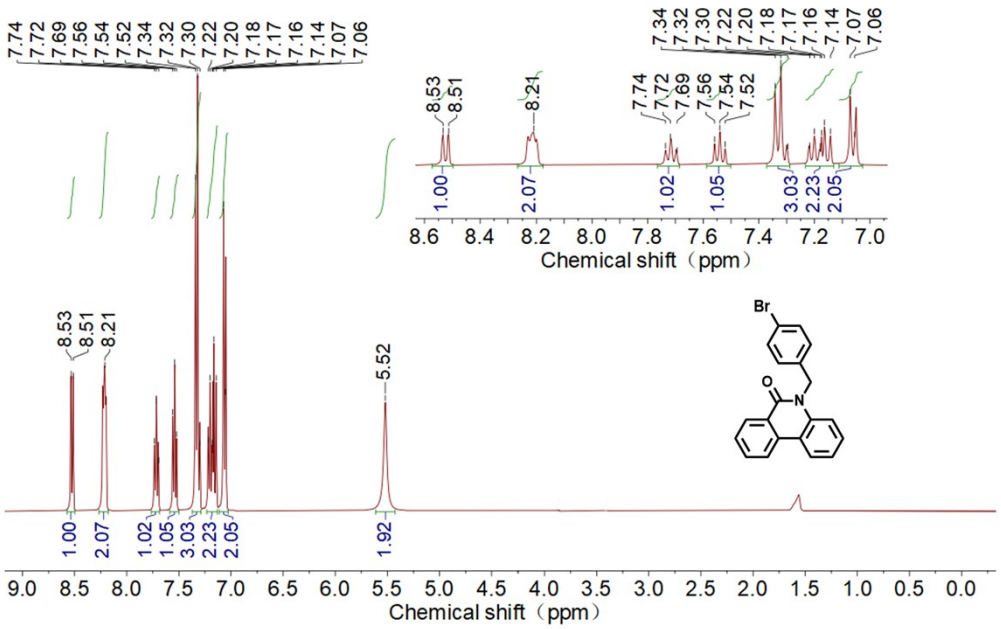

Figure S5. ^{1}H NMR spectrum of **PTD-BnBr** ($CDCl_3$, 400 MHz).

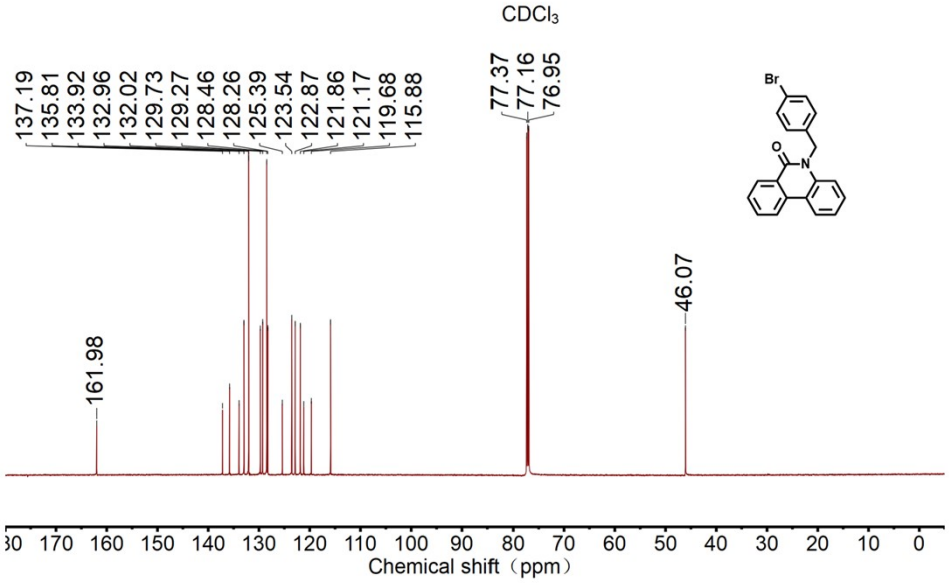

Figure S6. ^{13}C NMR spectrum of **PTD-BnBr** (151 MHz, $CDCl_3$).

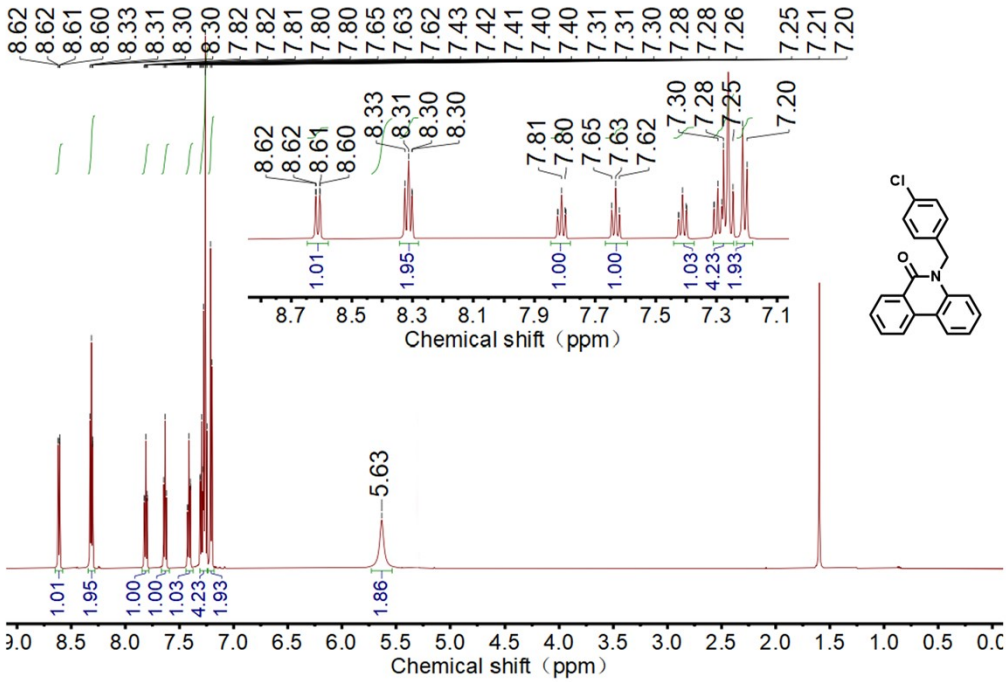

Figure S7. ^{1}H NMR spectrum of **PTD-BnCl** ($CDCl_3$, 400 MHz).

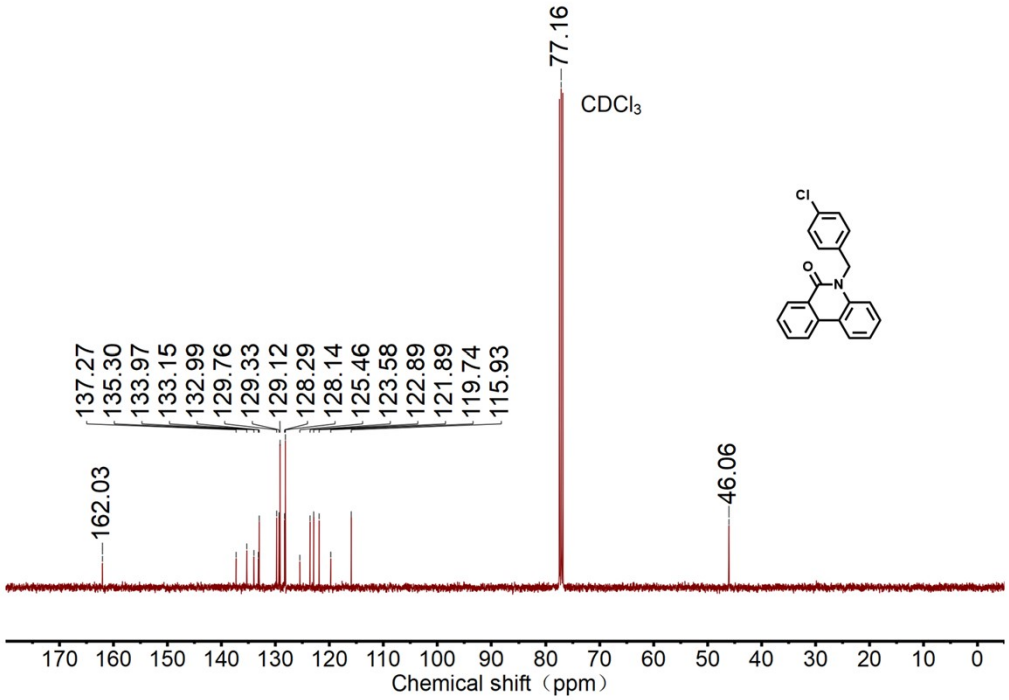

Figure S8. ^{13}C NMR spectrum of **PTD-BnCl** (101 MHz, $CDCl_3$).

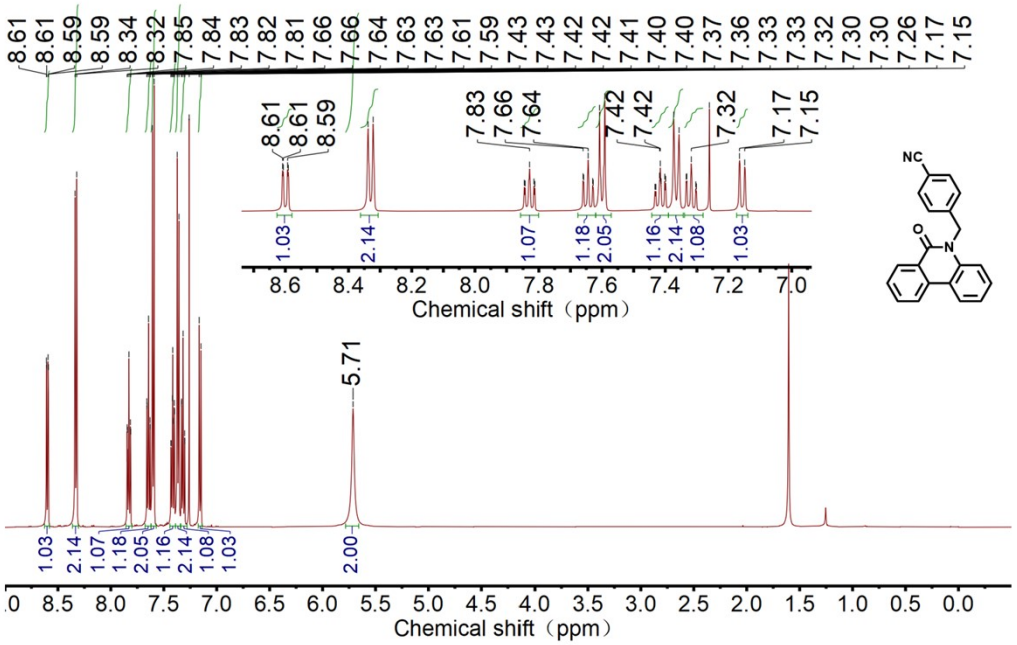

Figure S9. ^{1}H NMR spectrum of **PTD-BnCN** ($CDCl_3$, 500 MHz).

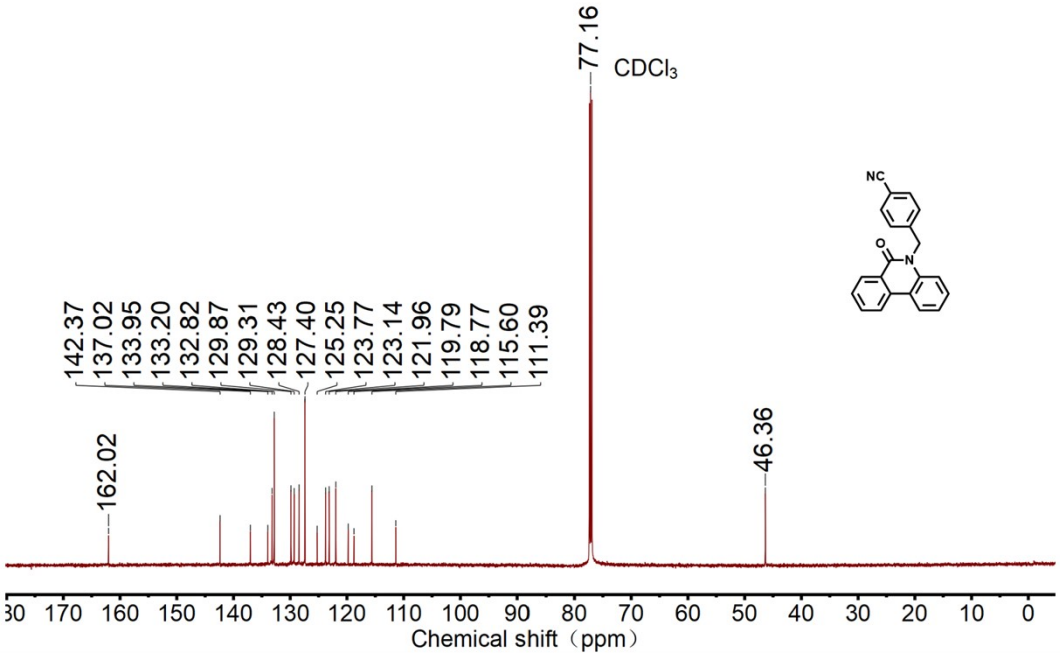

Figure S10. ^{13}C NMR spectrum of **PTD-BnCN** (151 MHz, $CDCl_3$).

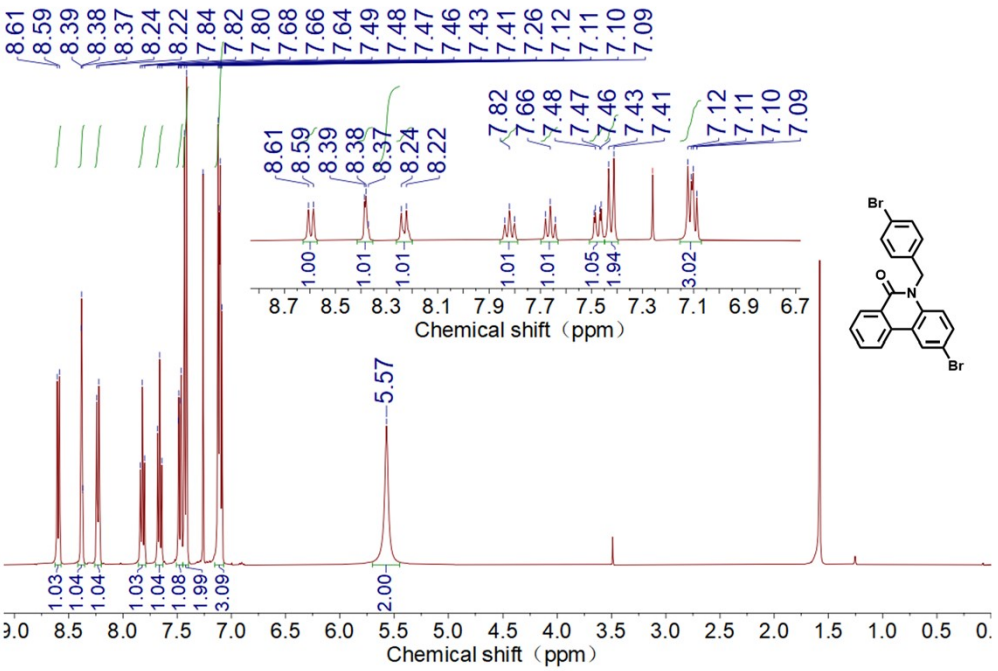

Figure S11. ^{1}H NMR spectrum of **Br-PTD** ($CDCl_3$, 400 MHz).

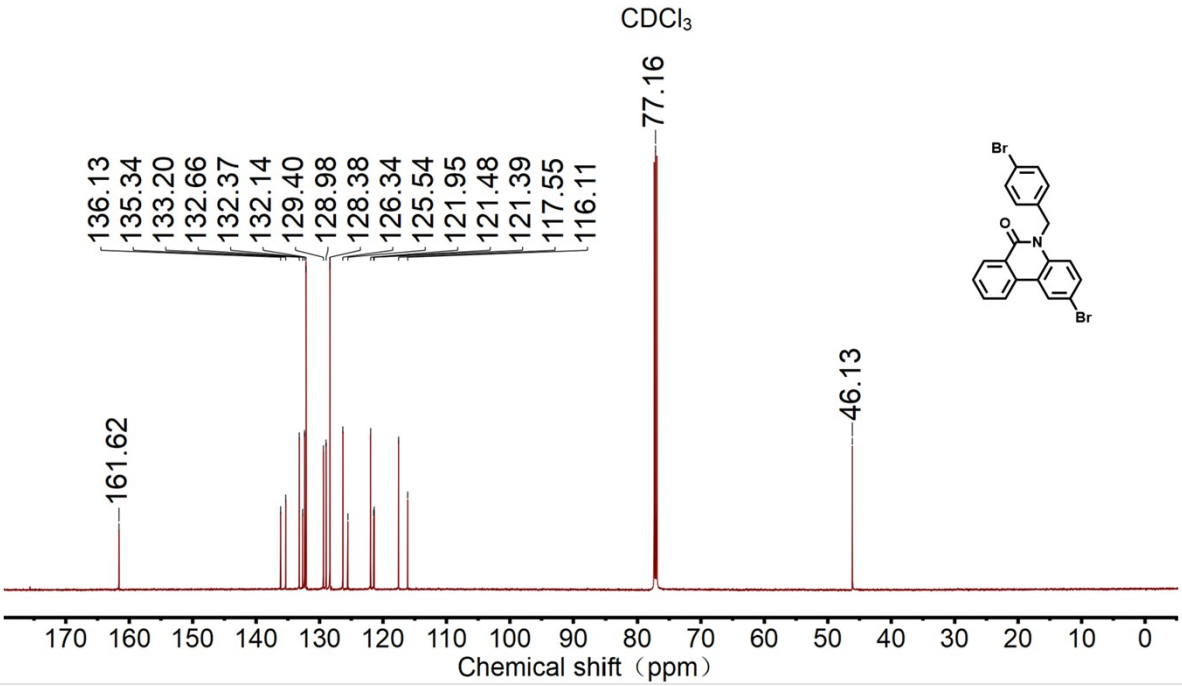

Figure S12. ^{13}C NMR spectrum of **Br-PTD** (151 MHz, $CDCl_3$).

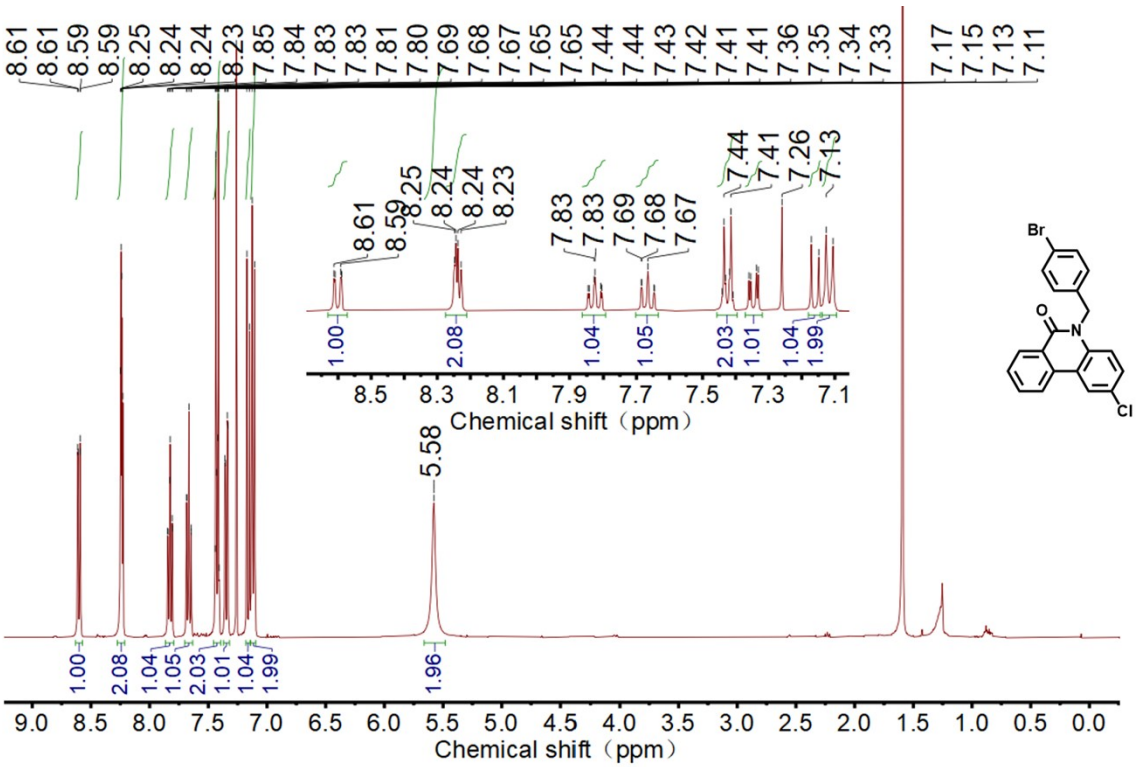

Figure S13. ^{1}H NMR spectrum of **Cl-PTD** ($CDCl_3$, 500 MHz).

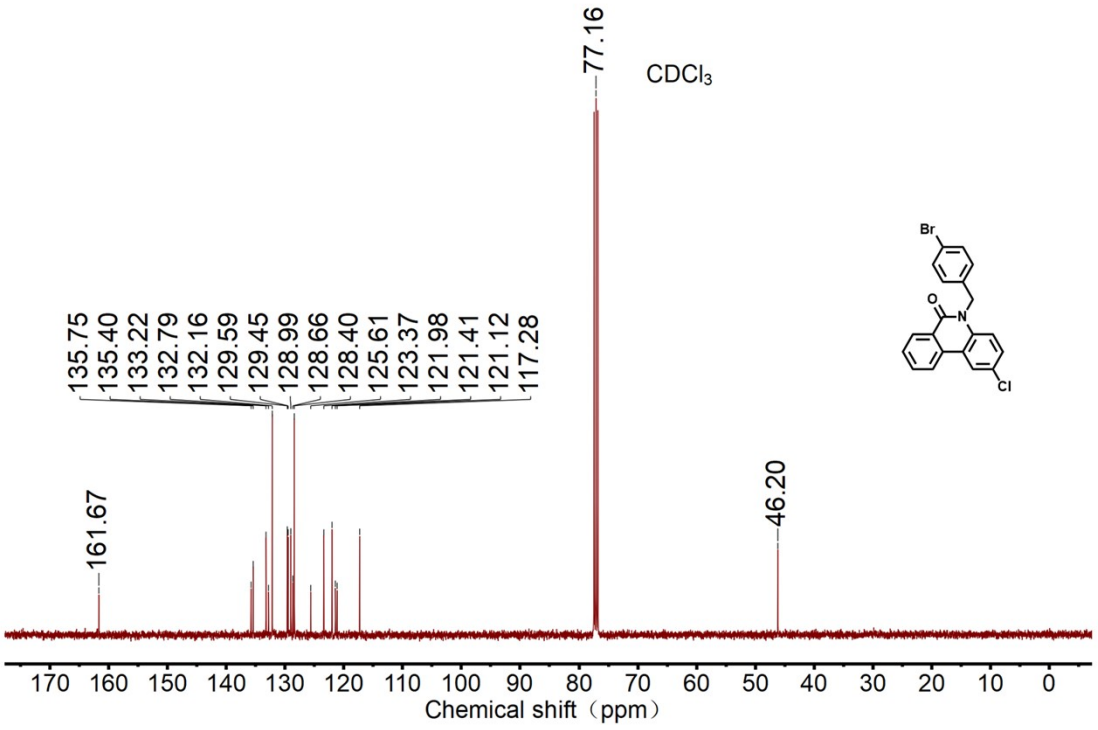

Figure S14. ^{13}C NMR spectrum of **Cl-PTD** (101 MHz, $CDCl_3$).

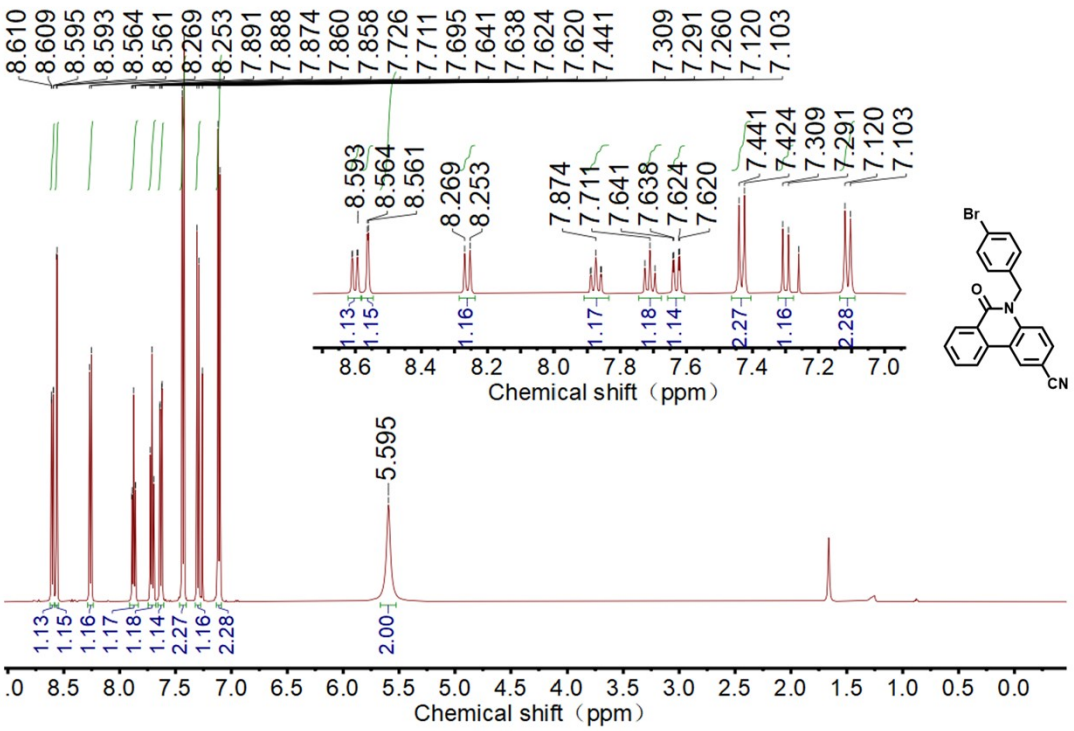

Figure S15. ^{1}H NMR spectrum of **CN-PTD** ($CDCl_3$, 500 MHz).

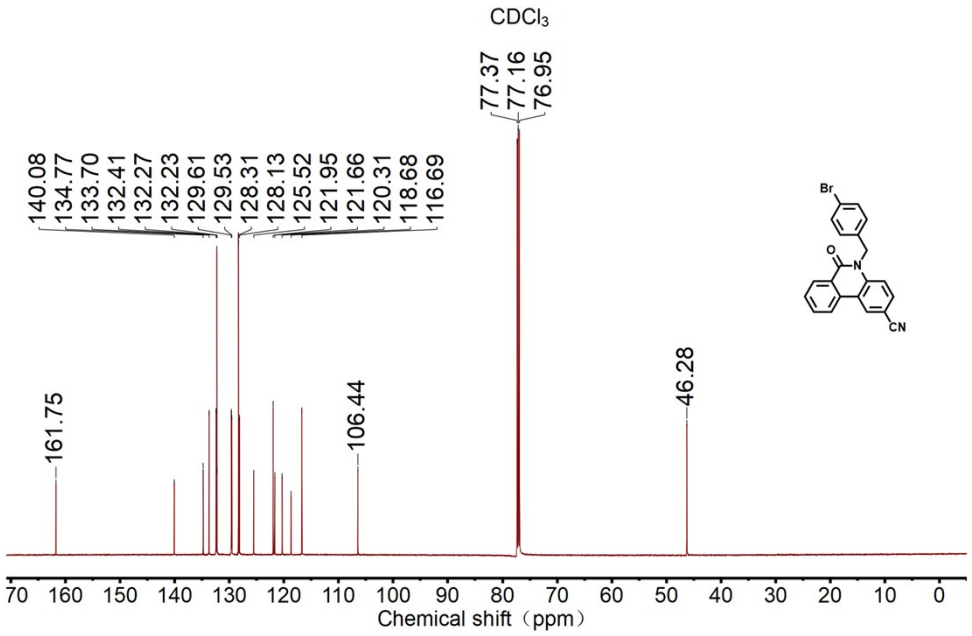

Figure S16. ^{13}C NMR spectrum of **CN-PTD** (151 MHz, $CDCl_3$).

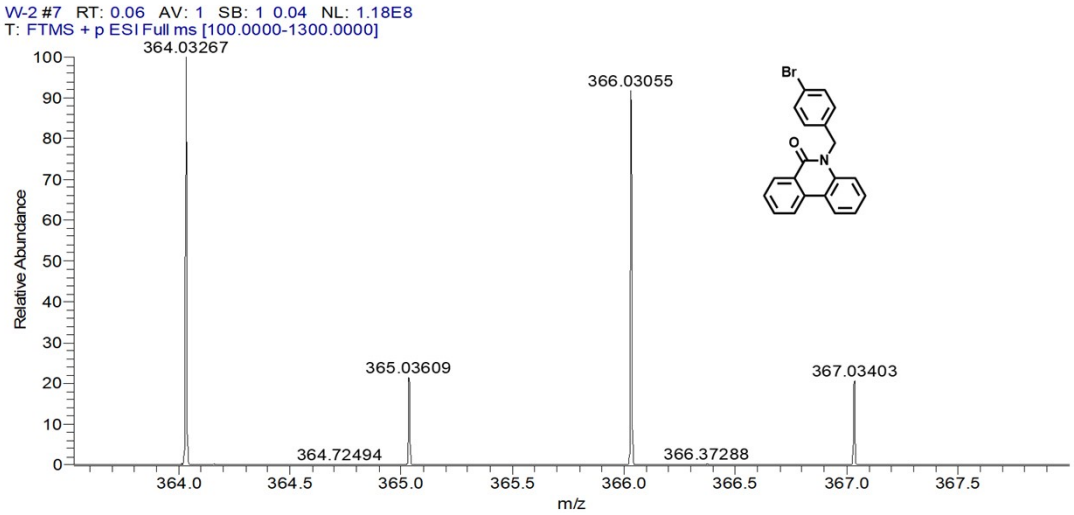

Figure S17. The ESI-HRMS spectrum of **PTD-BnBr**.

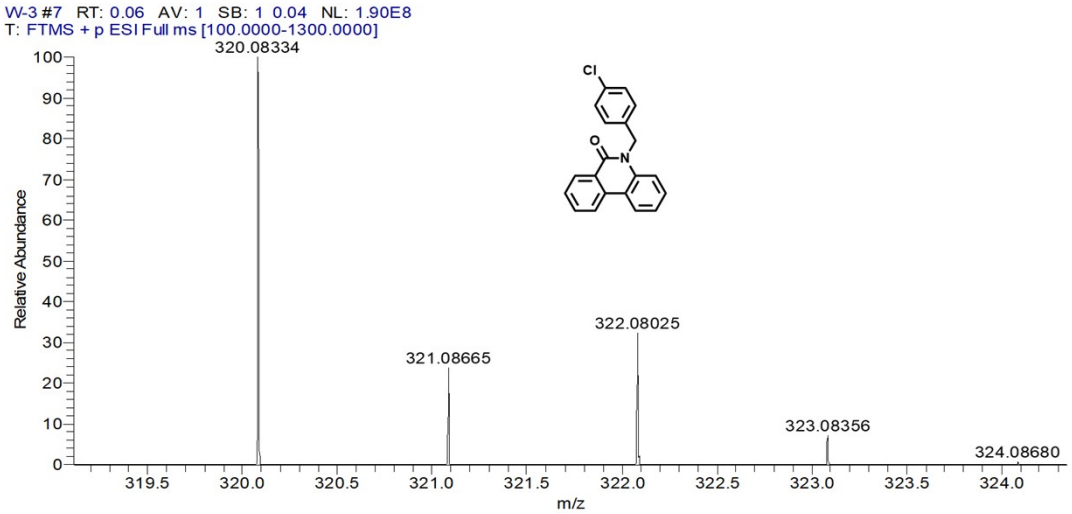

Figure S18. The ESI-HRMS spectrum of **PTD-BnCl**.

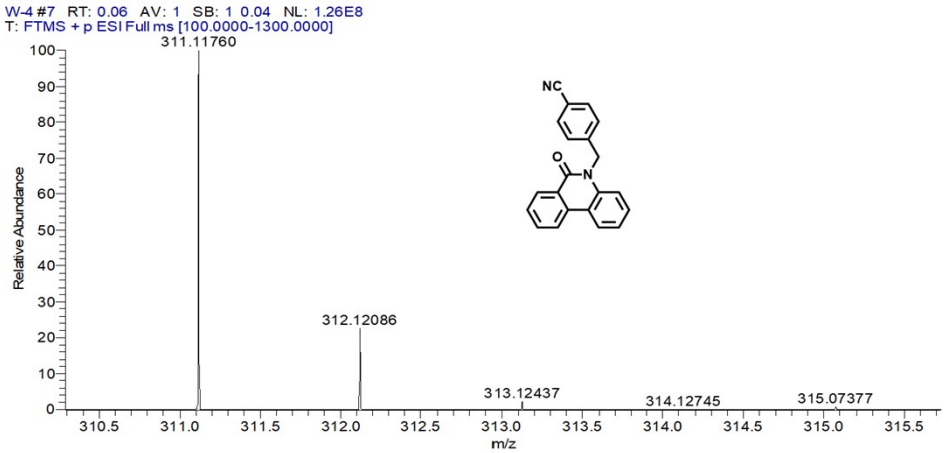

Figure S19. The ESI-HRMS spectrum of **PTD-BnCN**.

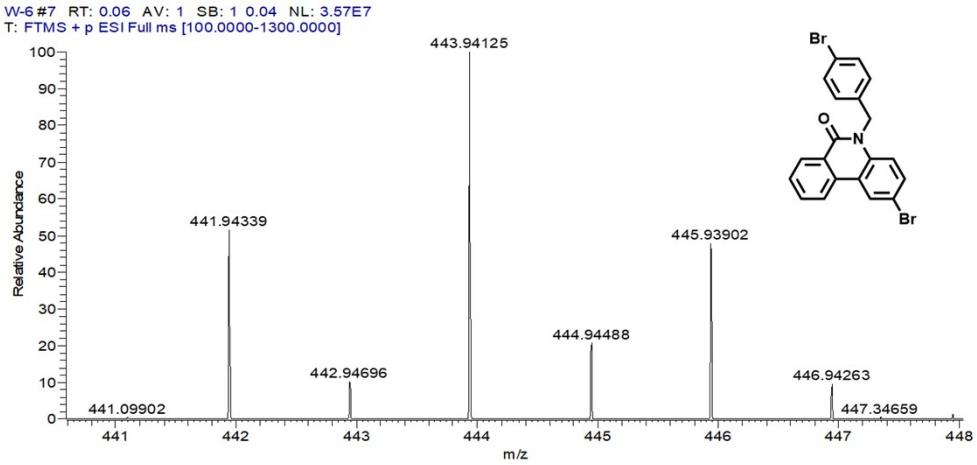

Figure S20. The ESI-HRMS spectrum of **Br-PTD**.

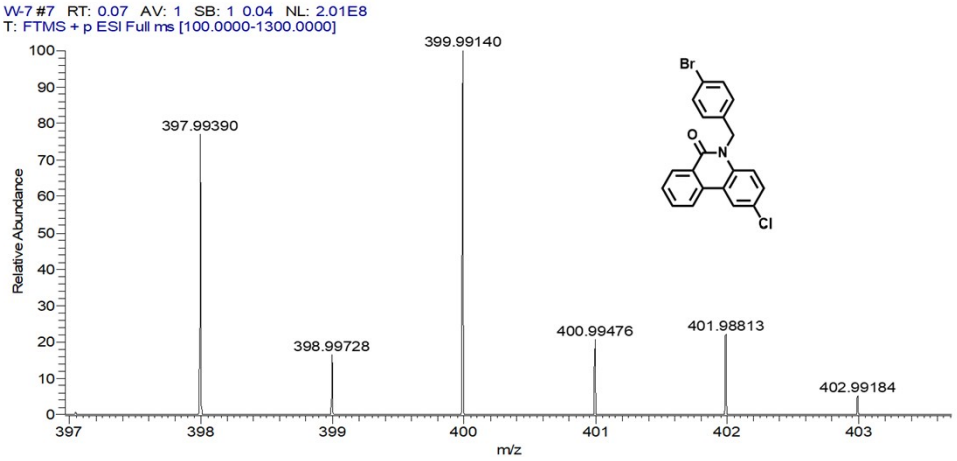

Figure S21. The ESI-HRMS spectrum of **Cl-PTD**.

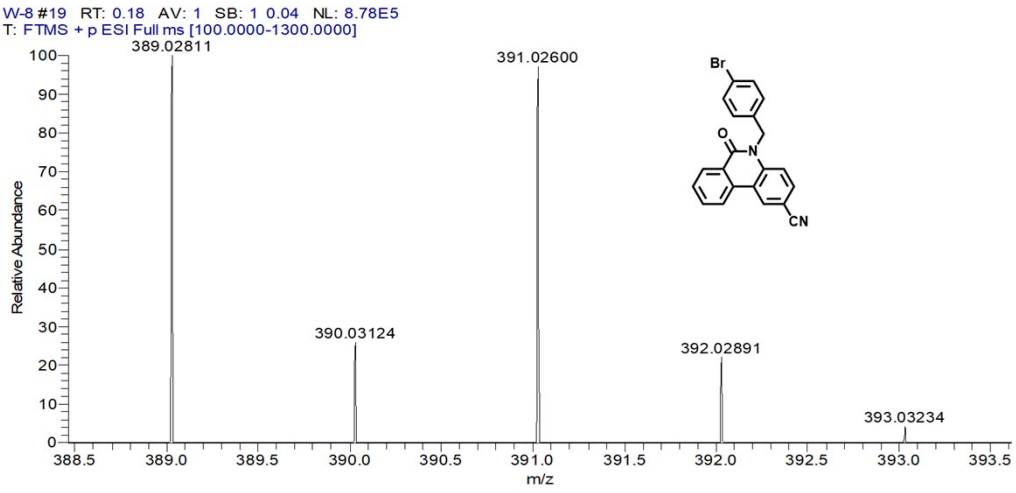

Figure S22. The ESI-HRMS spectrum of **CN-PTD**.

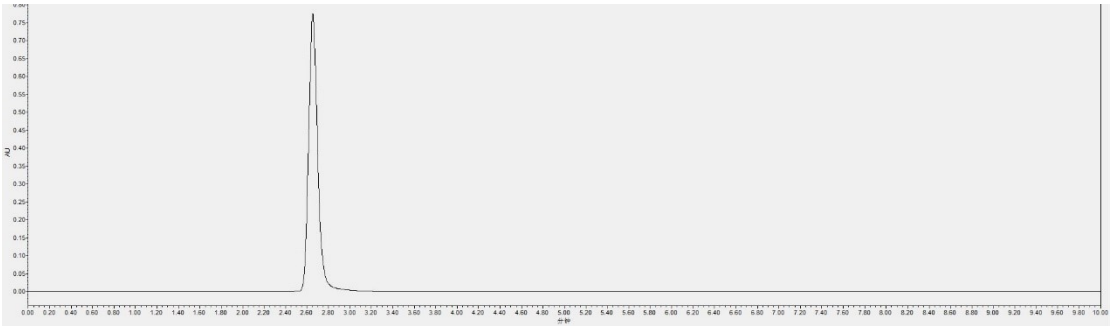

Figure S23. High-performance liquid chromatography diagram of **PTD-BnBr**.

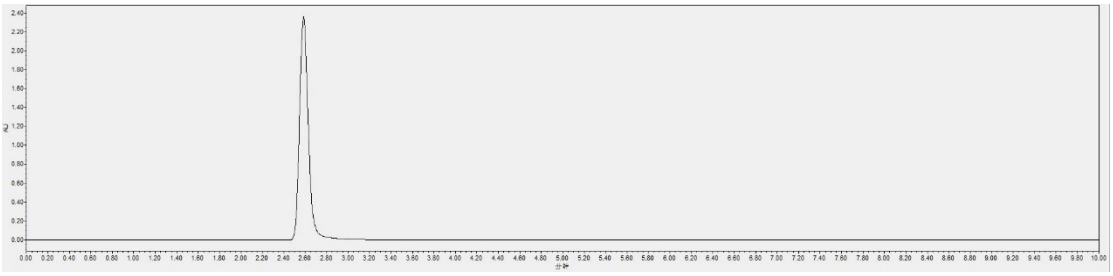

Figure S24. High-performance liquid chromatography diagram of **PTD-BnCl**.

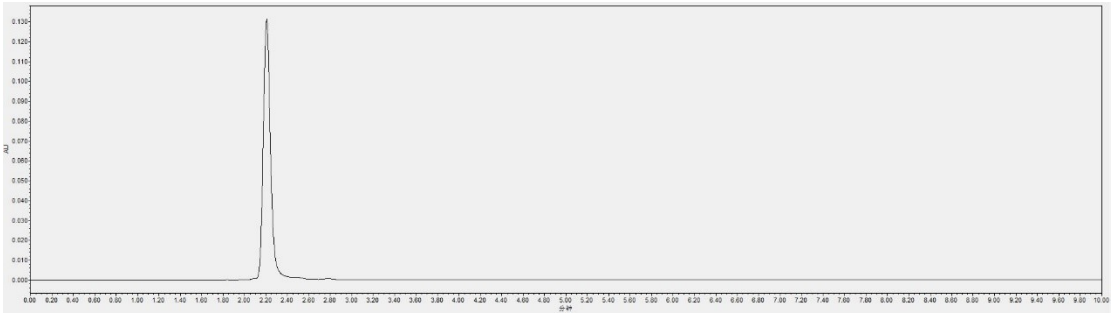

Figure S25. High-performance liquid chromatography diagram of **PTD-BnCN**.

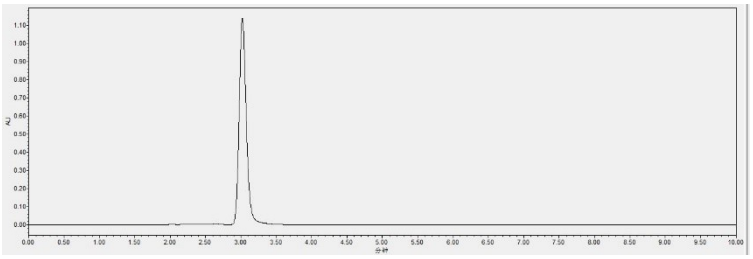

Figure S26. High-performance liquid chromatography diagram of **Br-PTD**.

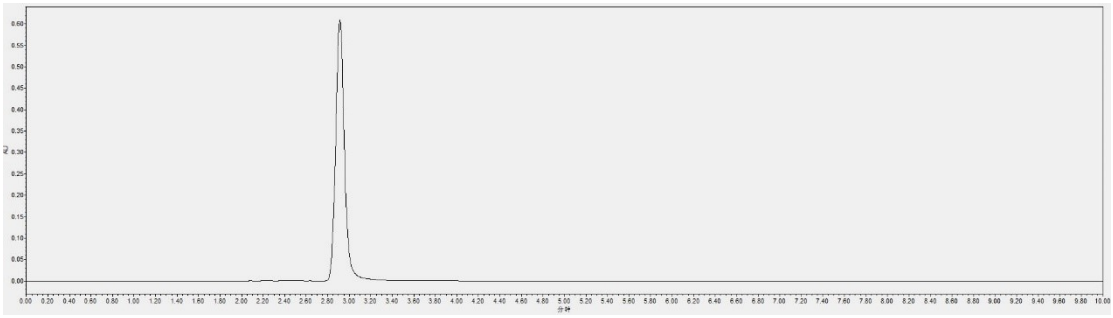

Figure S27. High-performance liquid chromatography diagram of **Cl-PTD**.

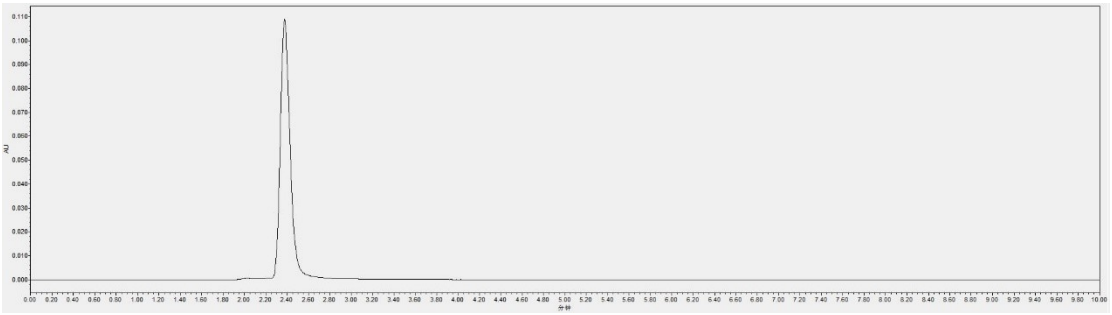

Figure S28. High-performance liquid chromatography diagram of **CN-PTD**.

References

[1] a) Dapprich, I. Komáromi, K. S. Byun, K. Morokuma, and M. J. Frisch. *J. Mol. Struct. (Theochem)*, **1999**, *462*,1-21. b) Chung, L. W.; Sameera, W. M. C.; Ramozzi, R.; Page, A. J.; Hatanaka, M.; Petrova, G. P.; Harris, T. V.; Li, X.; Ke, Z.; Liu, F.; Li, H.-B.; Ding, L.; Morokuma, K., The ONIOM Method and Its Applications. *Chem. Rev.,* **2015**, *115*, 5678-5796.

[2] Gaussian 09, Revision D.01, M. J. Frisch, G. W. Trucks, H. B. Schlegel, G. E. Scuseria, M. A. Robb, J. R. Cheeseman, G. Scalmani, V. Barone, B. Mennucci, G. A. Petersson, H. Nakatsuji, M. Caricato, X. Li, H. P. Hratchian, A. F. Izmaylov, J. Bloino, G. Zheng, J. L. Sonnenberg, M. Hada, M. Ehara, K. Toyota, R. Fukuda, J. Hasegawa, M. Ishida, T. Nakajima, Y. Honda, O. Kitao, H. Nakai, T. Vreven, J. A. Montgomery, Jr., J. E. Peralta, F. Ogliaro, M. Bearpark, J. J. Heyd, E. Brothers, K. N. Kudin, V. N. Staroverov, T. Keith, R. Kobayashi, J. Normand, K. Raghavachari, A. Rendell, J. C. Burant, S. S. Iyengar, J. Tomasi, M. Cossi, N. Rega, J. M. Millam, M. Klene, J. E. Knox, J. B. Cross, V. Bakken, C. Adamo, J. Jaramillo, R. Gomperts, R. E. Stratmann, O. Yazyev, A. J. Austin, R. Cammi, C. Pomelli, J. W. Ochterski, R. L. Martin, K. Morokuma, V. G. Zakrzewski, G. A. Voth, P. Salvador, J. J. Dannenberg, S. Dapprich, A. D. Daniels, O. Farkas, J. B. Foresman, J. V. Ortiz, J. Cioslowski, and D. J. Fox,

Gaussian, Inc., Wallingford CT, 2013.

[3] Patil, S.; Kamath, S.; Sanchez, T.; Neamati, N.; Schinazi, R. F.;Buolamwini, J. K., Synthesis and biological evaluation of novel 5(H)-phenanthridin-6-ones, 5(H)-phenanthridin-6-one diketo acid, and polycyclic aromatic diketo acid analogs as new HIV-1 integrase inhibitors. *Biorg. Med. Chem.,* **2007**, *15*, 1212-1228.

[4] Pan, H.-L.;Fletcher, T. L., 6(5H)-phenanthridinones. II. Preparation of substituted 6(5h)-phenanthridinones from 9-oxofluorenes. *J. Heterocycl. Chem.,* **1970**, *7*, 313-321.